Proceedings of the 2007 IEEE/RSJ International
Conference on Intelligent Robots and Systems
San Diego, CA, USA, Oct 29 - Nov 2, 2007

Estimating Viscoelastic Properties of Human Limb Joints Based on Motion Capture and Robotic Identification Technologies

Gentiane Venture, Katsu Yamane, Yoshihiko Nakamura, and Masaya Hirashima
The University of Tokyo - Department of Mechano-Informatics
7-3-1 Hongo Bunkyo-ku 113-8656 Tokyo Japan
{gentiane,yamane,nakamura,hirasima}@ynl.t.u-tokyo.ac.jp

***Abstract*— We present a solution to estimate in-vivo the joint dynamics of the human limbs during passive movements. The method is based on well-known modelling and approach used in Robotics that allow simultaneous multi-joint estimation. The modelling of the human body and the human joint as well as the method are described. The experimental set-up based on the use of an optical motion capture system is detailed. Three types of movements are recorded and used to perform the identification. We concluded that designed movements and movements from clinical diagnosis of neuromuscular diseases are good to perform the identification; however swing of the arms during normal walk does not provide enough excitation to obtain consistent results.**

I. Introduction

The study of dynamic motion of robotics systems often requires the simulation and the prediction of the system's behavior to avoid dangerous situations and to design appropriate controls. The simulators' reliability depends on the chosen model and on its parametrization to properly describe the real system. Usually the geometric parameters are easily measured directly on the system; however the dynamic parameters are difficult to measure directly and they are often unknown, even to manufacturers [1]. Identification is then a common approach to estimate these parameters of robot dynamics; several efficient techniques have been developed [1], [2], [3] and applied to complex systems [4], [5]. It is the same when dealing with human dynamics. To simulate human motion, to design ergonomic systems, and during clinical assessment of neuromuscular diseases, the knowledge of the dynamic properties and more particularly of the viscoelastic properties of the joints is crucial.

Biomechanics has successfully developed methodologies for measuring various dynamics properties of the human body [6], [7], [8]. The determination of standard values of joints' viscoelastic properties requires to have well calibrated measuring equipments and to average the data of many subjects. These equipments need mechanical stiffness and accuracy, which make them heavy and bulky in nature. Such equipments are unfortunately not applicable to everyone, specially those who are under rehabilitation and medical treatments. A system to measure the patient-specific viscoelastic properties of limb joints without pain and constraints is then useful.

In this paper we propose to identify the human limb dynamics using modelling and identification techniques developed for robots. This method offers a great flexibility in the description of the system and coupled with an optical motion capture studio it can provide an efficient painless and constraint-free tool to characterize the subject-specific dynamics. In the following sections we will present the modelling of the human body and the limb joints, then we briefly describe the obtention of the identification model and the identification method. In the third section we present the experimental background and state of the art before describing our original experimental set-up. Finally in the fourth section we give and discuss the obtained experimental results.

II. Modelling the human limbs

According to robotics modelling [1] the human body is described using two separate models. One model describes the kinematic structure and another one describes the dynamics of the limb joints. The kinematic structure of the human body is a simple rigid body model with 34 degrees of freedom (dof) as shown in Fig. 1. The details of the dof are given in Table I. Using this model, forward and inverse kinematics, and forward and inverse dynamics are computed according to [9] to give respectively the joint angles and the joint torques.

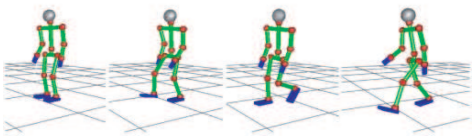

Fig. 1. A simplified model of the human body with 34 dof used to compute the human kinematics and dynamics from optical marker positions

Human limb joint viscoelastic properties are represented as torsion spring-damper systems [6]. They are the combination of the elasticity, viscosity and Coulomb frictions due to the

TABLE I

DEGREES OF FREEDOM IN THE MODEL OF THE HUMAN BODY

name of joint	type of joint	number of dof
neck	spherical	3
waist	spherical	3
right shoulder	spherical	3
right elbow	revolute	1
right wrist	spherical	3
left shoulder	spherical	3
left elbow	revolute	1
left wrist	spherical	3
right hip	spherical	3
right knee	revolute	1
right ankle	spherical	3
left hip	spherical	3
left knee	revolute	1
left ankle	spherical	3

passive musculo-tendon, the connective tissues and the soft tissues [10]. In the inverse dynamics, they are represented respectively by $\mathbf{\Gamma}^e$, $\mathbf{\Gamma}^v$ and $\mathbf{\Gamma}^f$ and the inverse dynamics can be written as follows:

$$\mathbf{\Gamma} + \boldsymbol{Q} = \boldsymbol{A}(\boldsymbol{q})\ddot{\boldsymbol{q}} + \boldsymbol{B}\left(\boldsymbol{q}, \dot{\boldsymbol{q}}\right) \tag{1}$$

$$\mathbf{\Gamma} + \boldsymbol{Q} = \mathbf{\Gamma}^e + \mathbf{\Gamma}^v + \mathbf{\Gamma}^f + \boldsymbol{H}\left(\boldsymbol{q}, \dot{\boldsymbol{q}}, \ddot{\boldsymbol{q}}, \boldsymbol{D}_P\right) \tag{2}$$

where:

- $\mathbf{\Gamma}$ is the vector of joint forces or torques due to actuation: in the human body actuation is due to contractions of antagonist muscles. For passive movements $\mathbf{\Gamma} = 0$.
- $\boldsymbol{Q}$ is the vector of generalized efforts representing the projection of the external forces and torques on the joint axes, it is calculated with:

$$\boldsymbol{Q} = -\sum \boldsymbol{J}_j(\boldsymbol{q})^T \boldsymbol{F}_{ej} \tag{3}$$

- j denotes the concerned joint in the chain and the following link attached to it,
- $\boldsymbol{J}_j(\boldsymbol{q})$ is the Jacobian matrix of the frame attached to body j
- $\boldsymbol{F}_{ej}$ is the vector of external forces and moments applied by body j on the environment,
- $\boldsymbol{q}$ is the vector of joint angles q_j, $\dot{\boldsymbol{q}}$ and $\ddot{\boldsymbol{q}}$ are its first and second time derivatives,
- $\boldsymbol{A}$ is the mass matrix of the system,
- $\boldsymbol{B}$ is the vector of Coriolis, centrifugal and gravity forces,
- $\boldsymbol{H}$ is the vector of inertial, Coriolis, centrifugal and gravity forces:

$$\boldsymbol{H}\left(\boldsymbol{q}, \dot{\boldsymbol{q}}, \ddot{\boldsymbol{q}}, \boldsymbol{D}_P\right) = \boldsymbol{A}(\boldsymbol{q})\ddot{\boldsymbol{q}} + \boldsymbol{B}\left(\boldsymbol{q}, \dot{\boldsymbol{q}}\right) \tag{4}$$

- $\boldsymbol{D}_P$ is the vector of inertial parameters of the system: mass, inertia, first moment of inertia (10 parameters per link j),
- $\mathbf{\Gamma}^e$ is the joint elastic torque due to the apparent elasticity of the joint. For link j, $\mathbf{\Gamma}_e$ is written as:

$$\Gamma_j^e = k_j(q_j - q_j^r) = k_j q_j + o_j \tag{5}$$

with k_j the stiffness, q_j^r the natural rest angle induced by gravity, $o_j = -k_j q_j^r$ the corresponding offset,

- $\mathbf{\Gamma}^v$ is the joint viscosity torque. With h_j the viscous coefficient:

$$\Gamma_j^v = h_j \dot{q}_j \tag{6}$$

- $\mathbf{\Gamma}^f$ is the friction torque. It is modelled by a Coulomb coefficient f_j:

$$\Gamma_j^f = f_j sign(\dot{q}_j) \tag{7}$$

By separating the known dynamics from the dynamics to identify we obtain a linear system in the n_p parameters to estimate: k_j, h_j, f_j, o_j for each of the n_j joints. The inertial parameters, $\boldsymbol{D}_P$, are assumed to be known as they are too small to be estimated at the same time. The system is sampled along a movement of n_e samples, to give the linear over-determinate system of Eq. (8) that is solved using the linear least square. The condition number of the observation matrix $\boldsymbol{W}$ and the relative standard deviation $\sigma_{\hat{X}_j}\%$ for each estimated parameter, i.e. each component of vector $\hat{\boldsymbol{X}}$, can be computed and used to interpret the results [4].

$$\boldsymbol{Y} = \boldsymbol{W}\left(\boldsymbol{q}, \dot{\boldsymbol{q}}, \ddot{\boldsymbol{q}}\right)\boldsymbol{X} + \boldsymbol{\rho} \tag{8}$$

where:

- $\boldsymbol{Y}$ is the $(n_e n_j \times 1)$ vector of joint torques,
- $\boldsymbol{W}$ is the $(n_e n_j \times n_j n_p)$ observation matrix (or regressor matrix),
- $\boldsymbol{\rho}$ is the $(n_e n_j \times 1)$ vector of modelling and measurements errors,
- $\boldsymbol{X}$ is the $(n_j n_p \times 1)$ vector of parameters to estimate,
- $\hat{\boldsymbol{X}}$ is the $(n_j n_p \times 1)$vector of estimates.

III. EXPERIMENTAL SET-UP AND EXPERIMENTS

A. State of the art

In biomechanics and medical literature, measurements of joint stiffness can be found [11], [12], [13], [14]; however the proposed apparatus are often not appropriate for identification of joint passive viscoelasticity [7]. For example methods based upon the use of torque-meters or in-house systems [6], [15]. They are bulky and costly machines, requiring many calibrations, and only single joint experiments can be achieved. Moreover systems where candidates are strapped on an apparatus that imposes an external torque to the limb create a stressful situation that generates involuntary contractions of muscles. Only experienced candidates can overcome this issue. These contractions bias the estimation of the joint passive dynamics as the movement is not strictly passive. In addition the joint stiffness k_j is influenced by the range of imposed force [7]; consequently systems where a force is applied on the candidate are not reliable. An experimental set-up avoiding all these shortcomings is then expressly required. With those objectives in mind we have designed a new experimental process allows one to record the human limbs

movement in a painless constraint free environment and to perform the identification of the limb joints passive dynamics in a large experimental context.

B. Experimental process

The solution we propose here is based on the realization of movements in an optical motion capture studio [16]. In fact the optical motion capture studio is a convenient, non invasive and painless way to measure the human body movements as well as insuring no interaction between the candidate and the system. The acquisition of movements is achieved with optical markers pasted on the body of the candidate at appropriate anatomical points. The motion is recorded by the in-house system constituted of 10 cameras that we use in a range of 30 fps to 200 fps. Upper body and lower body are treated separately as it is difficult to excite both passive dynamics at the same time. For an increased accuracy and limited artifact due soft tissues movements, the markers are positioned above anatomical points such as bones. They are labelled manually. The recording of the upper limbs requires 14 optical markers as shown in Fig. 2 and as described bellow for each side:

- 1 marker on the top of the shoulders (above the acromion),
- 2 markers on each side (lateral and medial) of the elbows,
- 2 markers on each side of the wrists (ulna's radial side and radius radial side),
- 1 marker on the top of the hands
- 1 marker on the hips is used to define the trunk posture, for a more accurate computation of the inverse kinematics.

For the recording of the lower limbs a similar number of markers is used as shown in Fig. 2.

As the performed movements need to be passive, we use a surface EMG system to check the activity of the muscles around the considered joints. It is only required as a verification: EMG data are not used for the identification and they are not required for a roll-out of the solution once it has been shown that the movements are passive.

C. Recorded movements for the identification

The movements used for the identification are painless, passive and constraint-free. We propose three kinds of movements for the upper limb and study the possibility of identifying the viscoelasticity of elbows and shoulders joints ($n_j = 4$) with each.

1) Free swing of the elbow: the first kind of movements is a free swing of the elbow as shown in Fig. 3-top. The shoulder is maintained at maximal extension with no abduction, the rest position of the elbow is about 90°. Before starting the test the forearm is lifted and maintained with maximal extension. When released, the forearm swings naturally around the rest position. These movements are an elbow joint equivalent of the knee joint pendulum tests first proposed in [11] and often used in medicine or biomechanics. Such movements are used as a basis as it will be shown that they guaranty a low condition number of the observation matrix and a good excitation of the parameters to be estimated.

2) Clinical diagnosis of neuromuscular diseases: the second kind of movements is a record of tests performed during the clinical assessment of neuromuscular diseases (Fig. 3)-center. Among the clinical tests, typical passive movements for the assessment of spasticity of the upper limbs are (1) the shake of the body by the shoulders (right) and (2) the lift and release of the arm letting them swing freely (left). In both cases the rest position corresponds to the natural standing position with the arms along the body. The possibilities of quantifying the joint dynamics during such types of movements is important as they still allow clinicians visual qualitative rating of spasticity.

3) Free swing of the arms while walking: finally the third kind of movements is recorded during walk of the candidate. When walking the arms are swinging passively (Fig. 3-bottom) and without any constraint, moreover it is an easy movement that can usually be achieved naturally

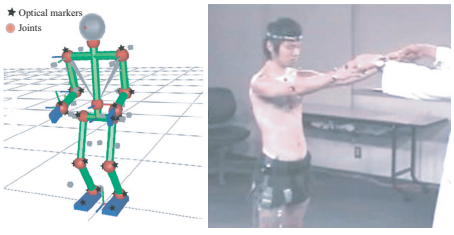

Fig. 2. Model with image of markers (left); candidate equipped with markers and EMG electrodes during experiments in the motion capture studio.

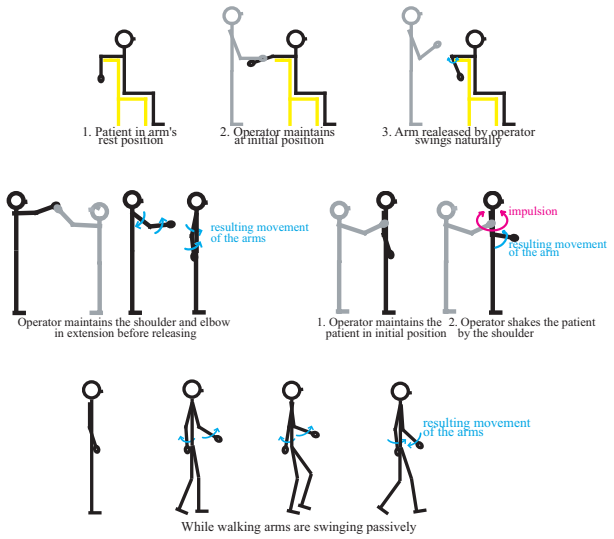

Fig. 3. The three kind of passive and constraint free movements used for the estimation: Free swing of the elbow (top), movements during medical diagnosis (center) and free swing of the arms while walking (bottom)

without stress. Studying the possibilities of performing the identification during such movements is then relevant. As the swing amplitude depends on the walk speed, walks in straight line at two different speeds: $3\,Km/h$ and $5\,Km/h$ are recorded. And walk on the tiptoe and on the heels are also recorded as they are sometimes used in clinical assessment of neuromuscular diseases.

IV. Experimental results

Three candidates of both genders (mean age 24 ± 3 years) received explanations of the purpose and procedure of the experimental process. Their upper body was equipped with 14 optical markers as described in section III-B. For each candidate the test described in section III-C.1 (that serves as a reference) was performed and recorded 4 to 6 times to insure a good repeatability. As mentioned in section III-B EMG were recorded too and are given in Fig. 4. For each candidates the tests were concatenated and the identification was performed using the whole data-set (about 1200 samples). Obtained results are given in Table II.

The second kind of tests was performed on candidate 2. Candidate was equipped with the same set of optical markers on the upper body. A clinician performed a complete clinical diagnosis typically used in the assessment of Parkinson disease as described in section III-C.2. The estimation was carried out using the different passive movements given in Fig. 3-center. The obtained results are in Table III.

The third kind of movements was recorded on candidate 2 with the same set of optical markers. Several types of walks were recorded such as in III-C.3. The identification was carried out concatenating all types of movements. The obtained results are given in Table IV.

A. Validation figures of the results

In addition to the computation of the condition number of $\boldsymbol{W}$ and the relative standard deviation for each estimated parameter $\sigma_{\hat{X}_j}\%$, the identification results are interpreted using validation figures. They consist in comparing the vector of joint torques $\boldsymbol{Y}$ with the joint torque estimated from joint angles and joints dynamics: $\boldsymbol{W}\hat{\boldsymbol{X}}$. The resulting error is also given: $\boldsymbol{Y} - \boldsymbol{W}\hat{\boldsymbol{X}}$. It is common to give *direct validations*, they consist in using a movement that was in the set of movements used for the identification (the error is then the vector of errors

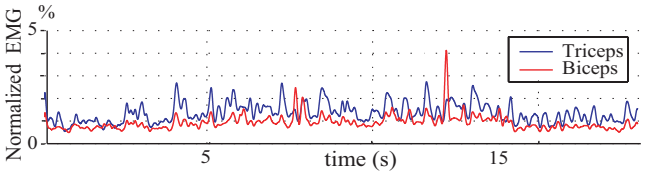

Fig. 4. EMG records of the Biceps and the Triceps to check the passivity of movements

TABLE II

Results of the estimation with free swing of the elbow

parameter	unit	$\hat{\boldsymbol{X}}$	$\sigma_{\hat{X}_j}\%$	$\hat{\boldsymbol{X}}$	$\sigma_{\hat{X}_j}\%$
Candidate 1					
shoulder		right		left	
$cond(\boldsymbol{W}_s)$		42		1382	
elbow		right		left	
$cond(\boldsymbol{W}_e)$		3.4		∞	
stiffness k_e	Nm/rad	2.61	0.3		
viscosity h_e	Nms/rad	0.05	7.7		
friction f_e	Nm	-0.02	25		
offset o_e	Nm	-0.04	9.8		
Candidate 2					
shoulder		right		left	
$cond(\boldsymbol{W}_s)$		57		403	
elbow		right		left	
$cond(\boldsymbol{W}_s)$		3.6		∞	
stiffness k_e	Nm/rad	2.24	0.3		
viscosity h_e	Nms/rad	0.03	9.4		
friction f_e	Nm	-0.01	20		
offset o_e	Nm	-0.01	15		
Candidate 3					
shoulder		right		left	
$cond(\boldsymbol{W}_s)$		49		808	
elbow		right		left	
$cond(\boldsymbol{W}_s)$		3.5		∞	
stiffness k_e	Nm/rad	2.17	0.2		
viscosity h_e	Nms/rad	0.02	13		
friction f_e	Nm	-0.003	68		
offset o_e	Nm	-0.01	18		

TABLE III

Results of the estimation for candidate 2 using diagnosis

parameter	unit	$\hat{\boldsymbol{X}}$	$\sigma_{\hat{X}_j}\%$	$\hat{\boldsymbol{X}}$	$\sigma_{\hat{X}_j}\%$
Candidate 2					
shoulder		right		left	
$cond(\boldsymbol{W}_s)$		2.96		2.57	
stiffness k_s	Nm/rad	9.53	0.73	7.88	0.87
viscosity h_s	Nms/rad	0.28	12.11	0.27	16.48
friction f_s	Nm	-0.25	13.34	0.02	154
offset $o_e s$	Nm	-2.22	1.37	-1.68	1.71
elbow		right		left	
$cond(\boldsymbol{W}_e)$		5.83		6.56	
stiffness k_e	Nm/rad	2.22	1.77	2.30	1.42
viscosity h_e	Nms/rad	0.36	5.30	0.18	9.98
friction f_e	Nm	-0.04	37.06	-0.12	10.64
offset o_e	Nm	-2.72	1.12	-3.12	1.02

ρ in (8)); and *cross validations* that consist in using any other movement that hasn't been used in the identification process.

B. Analysis of the results

As shown in the sequence of EMG in Fig. 4, during recorded movements there is less than 5% activation of the muscles around the concerned joint; the movements are consequently passive.

In the following, lower scripts "s" denotes the shoulder, "e" denotes the elbow, "r" the right side and "l" the left side.

1) Results for the first set of tests: we first consider the condition number for each joint. For the 3 candidates

TABLE IV

RESULTS OF THE ESTIMATION FOR CANDIDATE 2 USING NORMAL WALK

parameter	unit	$\hat{\boldsymbol{X}}$	$\sigma_{\hat{X}_j}\%$	$\hat{\boldsymbol{X}}$	$\sigma_{\hat{X}_j}\%$
Candidate 2					
shoulder		right		left	
$cond(\boldsymbol{W}_s)$		10.39		8.83	
stiffness k_s	Nm/rad	20.58	3.43	17.13	3.06
viscosity h_s	Nms/rad	-0.48	33.08	-0.01	800.32
friction f_s	Nm	0.28	0.24	0.23	37.09
offset o_es	Nm	-2.59	5.11	-2.13	4.19
elbow		right		left	
$cond(\boldsymbol{W}_e)$		9.40		10.16	
stiffness k_e	Nm/rad	3.14	3.49	4.01	2.72
viscosity h_e	Nms/rad	0.13	29.1	0.28	13.50
friction f_e	Nm	0.10	33.1	0.05	59.33
offset o_e	Nm	-3.79	3.11	-4.74	2.33

$cond(\boldsymbol{W}_{sr,l}) \gg 5$ and $cond(\boldsymbol{W}_{el}) = \infty$ which means that $cond(\boldsymbol{W})$ for these joints is ill-conditioned and that the parameters of both shoulders and of the left elbow can't be estimated. This was expected as in those movements the shoulders and the left elbow are not moving, their dynamics are consequently not excited. For each candidate $cond(\boldsymbol{W}_{er}) < 5$, which certify a well-conditioned observation matrix. The stiffness k_{er} of the right elbow joint is estimated with good accuracy according to the low value of the relative standard deviation $\sigma_{\hat{X}_{k_{er}}\%} < 1$. The joint viscosity h_{er} is also estimated for candidates 1 and 2 with good accuracy: $\sigma_{\hat{X}_{h_{er}}\%} < 10$; for candidate 3 the value of the parameter is low and $\sigma_{\hat{X}_{h_{er}}\%} > 10$ which makes it hard to conclude, however the likeness of the value compared to the ones obtained for the other candidates allows admitting that the range is correct. For the friction f_{er} the estimated value is low. Consequently the relative standard deviation becomes $\sigma_{\hat{X}_{f_{er}}\%} > 10$. It is then difficult to conclude from analyzing $\sigma_{\hat{X}_{f_{er}}\%}$. However according to the similarity of the results for the three candidates we can note that friction in the elbow joint is less than 5% of the joint torque. In addition, obtained results are confirmed by the validation given in Fig. 5.

2) Results for the second set of tests: During the clinical diagnosis both arms dynamics are excited. Condition numbers of $\boldsymbol{W}_{e,s}$ are lower or about 5, which guaranties a good simultaneous excitation of the dynamics for the four joints. From the analysis of $\sigma_{\hat{X}_j}$ for each parameter we obtain the same conclusions as in the first case. Stiffness is well estimated, viscosity of the elbow is fair, and viscosity of the shoulders and friction for the four joints are small; consequently, it is hard to draw conclusions from the relative standard deviations. The comparison of the obtained $k_e$using the clinical tests with k_{re} given in Table II is consistent as there is less than 0.01% error. The direct and cross validations are given in Fig. 6 and 7. From validations we can see that when the joint is reaching boundaries the error is increased. This can be due to a failure of the linear model in describing the joint properties at the boundaries [17]. In [16] results for the elbow are compared with literature.

3) Results for the third set of tests: The observation matrices obtained during the natural walk are such that $cond(\boldsymbol{W}_{e,s}) \gg 5$. It means that the movements don't guaranty a good excitation of the dynamics to be estimated, and consequently, the obtained parameters are not reliable. While walking the arms are swinging freely, however the range of motion for the recorded movements is at least 2 times smaller

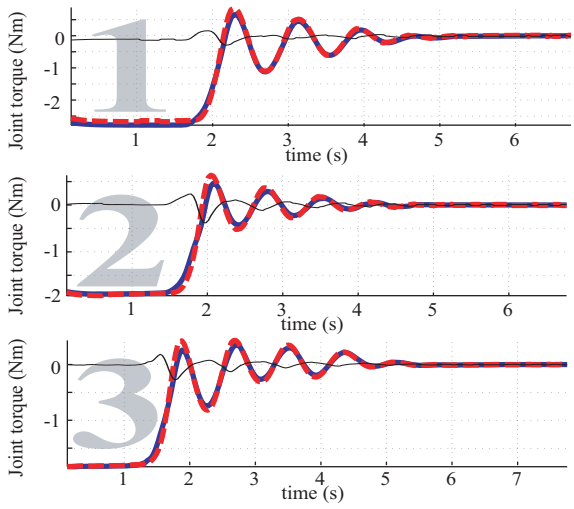

Fig. 5. Direct validation for the three patients. Vector of joint torques $\boldsymbol{Y}$ (thick blue line), estimated joint torque: $\boldsymbol{W}\hat{\boldsymbol{X}}$ (thick red dotted line) and error $\boldsymbol{Y} - \boldsymbol{W}\hat{\boldsymbol{X}}$ (thin black dotted line)

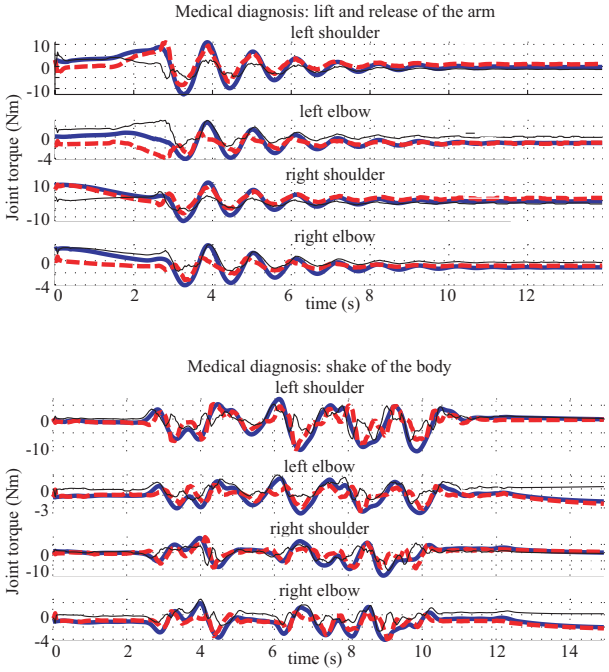

Fig. 6. *Direct validations* with clinical diagnosis movements (lift and release of the arms (top), shake of the body (bottom)). Same legend as Fig. 5.

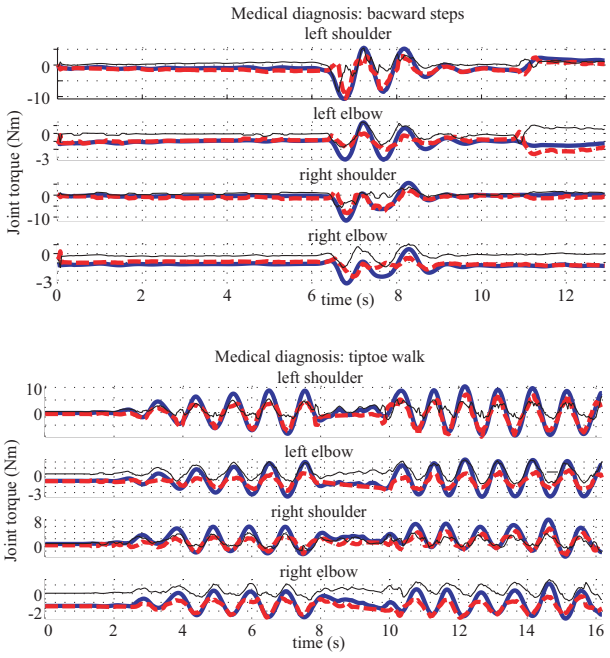

Fig. 7. *Cross validations*: clinical diagnosis movements are used for the identification and walk movements (backward steps (top) and tiptoe6 walk (bottom) are used for validations. Same legend as Fig. 5.

than with the other movements. But these movements can be used for cross validations as in Fig. 7.

V. Conclusion

Using robotics identification technology we have estimated the human limb's joints viscoelastic properties during passive movements. The movements are recorded by an optical motion capture system. It offers several advantages over conventional measuring devices used for this kind of applications. It is non invasive, painless, there is no contact with the candidate which avoids stressful situations and it allows constraint-free movements in the full range of motion. It can record the movements of all the limbs simultaneously. We have shown here that movements with enough amplitude and exciting properties, ie $cond\, \boldsymbol{W} \leq 5$ can be used to estimate the viscoelasticity of the upper limbs joints. Which is the case with those especially designed and with those from clinical diagnosis of neuromuscular diseases. The stiffness, the offsets, and the elbow viscosities are estimated with good accuracy as $\sigma_{\hat{X}j} \leq 10\%$. Results obtained using whether one set of movements or the other are confirmed as the difference between the two estimated stiffness k_{re} is lower than 0.01%; and also by the validation figures. However when using the swings of the arms while walking the results are inconsistent as the observation matrices are ill-conditioned: $cond\, \boldsymbol{W} \gg 5$. These results are of great importance to provide a simple-to-use quantification tool of spasticity for neurologists, and for robotic prosthesis designers. Future works will focus (1) on estimating the lower limb joints to offer a full body estimation, (2) using these results as a base to enhance understanding of active movements.

Acknowledgement

The authors thank Dr. Tomotaka Yamamoto from the Tokyo University Hospital for his valuable comments on the clinical issues. This research was supported by JSPS grant in Aid No 17200012 and the Special Coordination Funds for Promoting Science and Technology: "IRT Foundation to Support Man and Aging Society".

References

[1] W. Khalil and E. Dombre, *Modeling, identification and control of robots*, Hermès Penton, London-U.K, 2002.

[2] M. Gautier, "Dynamic identification of robots with power model," in *Proc. Int. Conf. on Robotics and Automation, Albuquerque, USA*, 1997, pp. 1922–1927.

[3] J. Swevers, C. Ganseman, D. Bilgin, J. De Schutter, and H. Van Brussel, "Optimal robot excitation and identification," *IEEE Trans. on Robotics and Automation*, vol. 13, no. 5, pp. 730–740, 1997.

[4] G. Venture, P.J. Ripert, W. Khalil, M. Gautier, and P. Bodson, "Modeling and identification of passenger car dynamics using robotics formalism," *IEEE Transactions on Intelligent Transportation Systems*, vol. 7, no. 3, pp. 349–359, September 2006.

[5] P. Aarnio, K. Koskinen, and S. Salmi, "Simulation of the hybtor robot," in *Proc. of the 3rd Int. Conf. on Climbing and Walking Robots, Madrid, Spain*, Professional Engineering Publishing Ltd, Ed., 2000, pp. 267–274.

[6] A.C. Oatis, "The use of a mechanical model to describe the stiffness and damping characteristics of the knee joint in healthy adults," *PHYS THER*, vol. 73, no. 11, pp. 740–749, 1993.

[7] A. Prochazka, D.J. Bennett, M.J. Stephens, R. Sears-Duru, T. Roberts, and J.H. Jhamandas, "Measurement of rigidity in parkinson's disease," *Movement Disorders*, vol. 12, pp. 24–32, 1997.

[8] S. Stroeve, "Impedance characteristics of a neuromusculoskeletal model of the human arm i. posture control," *Biol. Cybern.*, vol. 81, pp. 475–494, 1999.

[9] Y. Nakamura and K. Yamane, "Dynamics computation of structure-varying kinematic chains and its application to human figures," *IEEE Trans. on Robotics and Automation*, vol. 16, no. 2, pp. 124–134, 2000.

[10] R.J. Johns and V. Wright, "Relative importance of various tissues in joint stiffness," *J Appl Physiol*, vol. 17, no. 5, pp. 824–828, 1962.

[11] R. Wartenberg, "Pendulousness of the leg as a diagnostic test," *Neurology*, vol. 1, pp. 18 – 24, 1951.

[12] S. Stroeve, "Learning combined feedback and feedward control of a musculoskeletal system," *Biol. Cybern.*, vol. 75, pp. 73–83, 1996.

[13] D.G. Lloyd and T.F. Bessier, "An emg-driven musculoskeletal model to estimate muscle forces and knee joint moment in vivo," *Journal of Biomechanics*, , no. 36, pp. 765–776, 2003.

[14] R.S. Valle, A. Casabona, R. Sgarlata, R. Garozzo, M. Vinci, and M. Cioni, "The pendulum test as a tool to evaluate passive knee stiffness and viscosity of patients with rheumatoid arthritis," *BMC Musculoskeletal Disorder*, vol. 7, pp. 89–100, 2006.

[15] F. Mobasser and K. Hashtrudi-Zaad, "A method for online estimation of human arm dynamics," in *Proceedings of the 28th IEEE EMBS Annual International Conference, New York City, USA*, 2006, pp. 2412–2416.

[16] G. Venture, K. Yamane, and Y. Nakamura, "In-vivo estimation of the human elbow joint dynamics during passive movements based on the musculo-skeletal kinematics computation," in *IEEE/Int. Conf. on Robotics and Automation*, Orlando, USA, May 2006, pp. 2960–2965.

[17] J.M. Winters and L. Stark, "Analysis of fundamental human movement patterns through the use of in-depth antagonistic muscle model," *IEEE Trans. on Biomedical Engineering*, vol. 32, no. 10, pp. 826–839, 1985.